JOC The Journal of Organic Chemistry

Article

pubs.acs.org/joc

Synthesis of a Double-Spanned Resorc[4]arene via Ring-Closing Metathesis and Calculation of Aggregation Propensity

Francesca Ghirga,[†] Deborah Quaglio,[†] Valentina Iovine,[†] Bruno Botta,*[,†] Marco Pierini,*[,†] Luisa Mannina,[†] Anatoly P. Sobolev,[‡] Franco Ugozzoli,[§] and Ilaria D'Acquarica*[,†]

[†]Dipartimento di Chimica e Tecnologie del Farmaco, Sapienza Università di Roma, p.le Aldo Moro 5, 00185 Roma, Italy

[‡]Laboratorio di Risonanza Magnetica "Annalaura Segre", Istituto di Metodologie Chimiche CNR Area della Ricerca di Roma, Via Salaria km 29.300, 00015 Monterotondo, Italy

[§]Dipartimento di Chimica, Università degli Studi di Parma, Parco Area delle Scienze 17/a, 43124 Parma, Italy

Supporting Information

ABSTRACT: Ring-closing metathesis (RCM) catalyzed by a second-generation Grubbs catalyst has been used to synthesize resorc[4]arenes **2b**−**5b** starting from undecenyl resorc[4]arene **1b** fixed in the cone conformation. X-ray diffraction analysis of the major metathesis product, **3b** (50% yield), revealed a cavity-shaped architecture resembling a basket, endowed with a large intramolecular space (∼10 Å) and a strong propensity to self-assemble as a supramolecular trio of heterochiral dimers. This prompted us to investigate the aggregation propensity of basket **3b** in THF/water solution by UV−visible spectroscopy. The cavitation Gibbs free-energy change ($\Delta\Delta G_{cav}$ = 4.78 kcal mol^{-1}) associated with the self-assembly of macrocycle **3b** was calculated as a measure of the solvophobic interactions involved in the process.

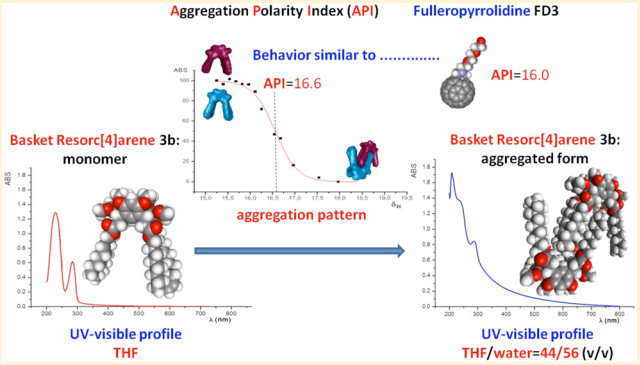

INTRODUCTION

Host preorganization is a key concept in supramolecular and materials chemistry because it represents the first step in envisaging any interaction with a range of complementary guests.[1] The most common approach toward preorganization of a host molecule is to increase the rigidity of its scaffold with the purpose of limiting the conformational degree of freedom available.[1,2] As a rule, the creation of properly rigidified macrocycles requires complex synthesis routes, including the preparation of suitable templates to be covalently[3] or noncovalently[4] linked to the reactant species. Olefin metathesis[5] recently proved a very efficient route to achieve the synthesis of a range of novel cage calixarenes,[6,7] the synthesis of huge macrocycles with more than 100 atoms,[8] and the formation of high-molecular-weight elastomers.[9] In 2013, we reported the synthesis of complex cyclic alkenes obtained by both intramolecular and intermolecular metathesis reactions of conformationally flexible resorc[4]arenes functionalized at the lower rim with vinylidene groups.[10] According to changes in the different reaction conditions, mainly catalyst loading, the terminal alkenes of two isolated chains of the macrocycle in the chair conformation underwent both intramolecular ring-closing metathesis (RCM) and intermolecular acyclic diene metathesis (ADMET) reactions.

We report the results obtained with the cone stereoisomer of the aforementioned resorc[4]arene, in which the four side chains are all cis (rccc). In fact, although in the chair conformation the side chains were isolated two by two on opposite sides of the molecule and reacted independently, in the case of the cone conformation the proximity of the four side chains induced by the conformation allowed us to synthesize double-spanned resorc[4]arene **3b** as a potential preorganized host. Later, we became interested in studying the aggregation propensity exhibited in X-ray diffraction analysis of a crystal of **3b**, so we developed a set of physical descriptors that, taken together, allowed us to calculate the hydrophilic−hydrophobic balance of the macrocycle.

RESULTS AND DISCUSSION

We recently synthesized undecenyl resorc[4]arenes **1a**, **1b**, and **1c** (Chart 1) by the tetramerization of (*E*)-2,4-dimethoxycinnamic acid *ω*-undecenyl ester with ethereal BF_3; these three molecules possess chair, cone, and 1,2-alternate conformations, respectively.[10] Resorc[4]arene **1a**, which features the simplest pattern of substituents (two isolated side chains with the other two substituents on the symmetric counterpart), was chosen for initial carrying out of an olefin metathesis reaction.[5] We next turned our attention to resorc[4]arene **1b**, in which the four side chains are all cis (rccc) in the lower part of the macrocycle.

Received: September 5, 2014
Published: October 21, 2014

   dx.doi.org/10.1021/jo502056v | J. Org. Chem. 2014, 79, 11051−11060

Chart 1. Chemical Structures of Previously Synthesized Resorc[4]arene ω-Undecenyl Esters 1a (chair), 1b (cone), and 1c (1,2-alternate)[10]

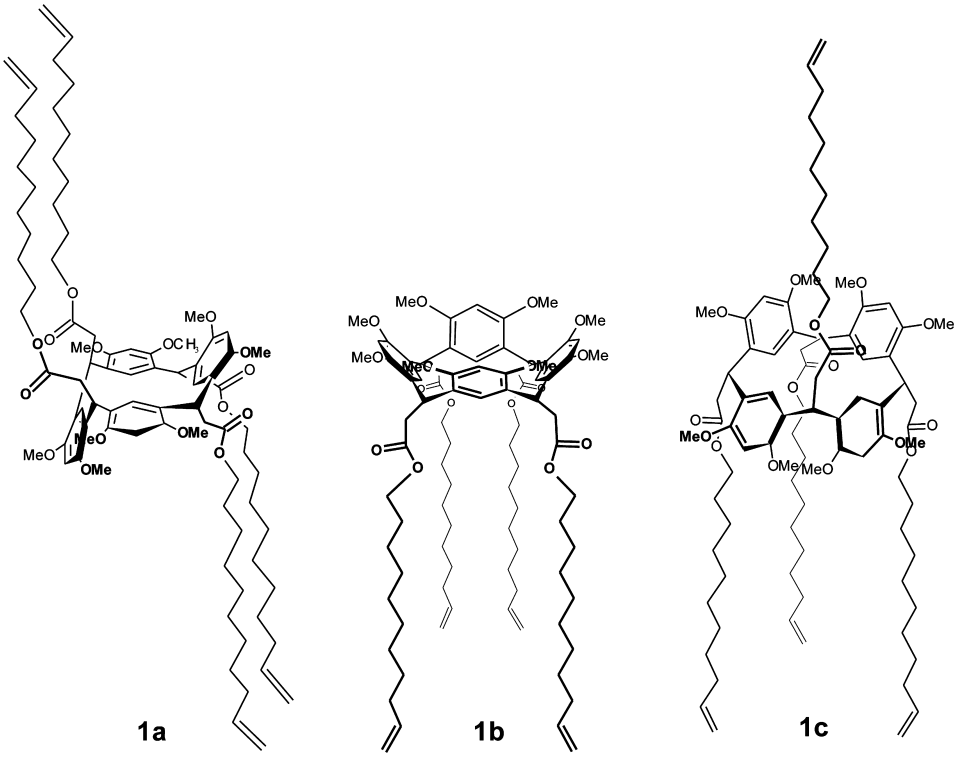

Scheme 1. Olefin Metathesis Reaction on Undecenyl Resorc[4]arene 1b

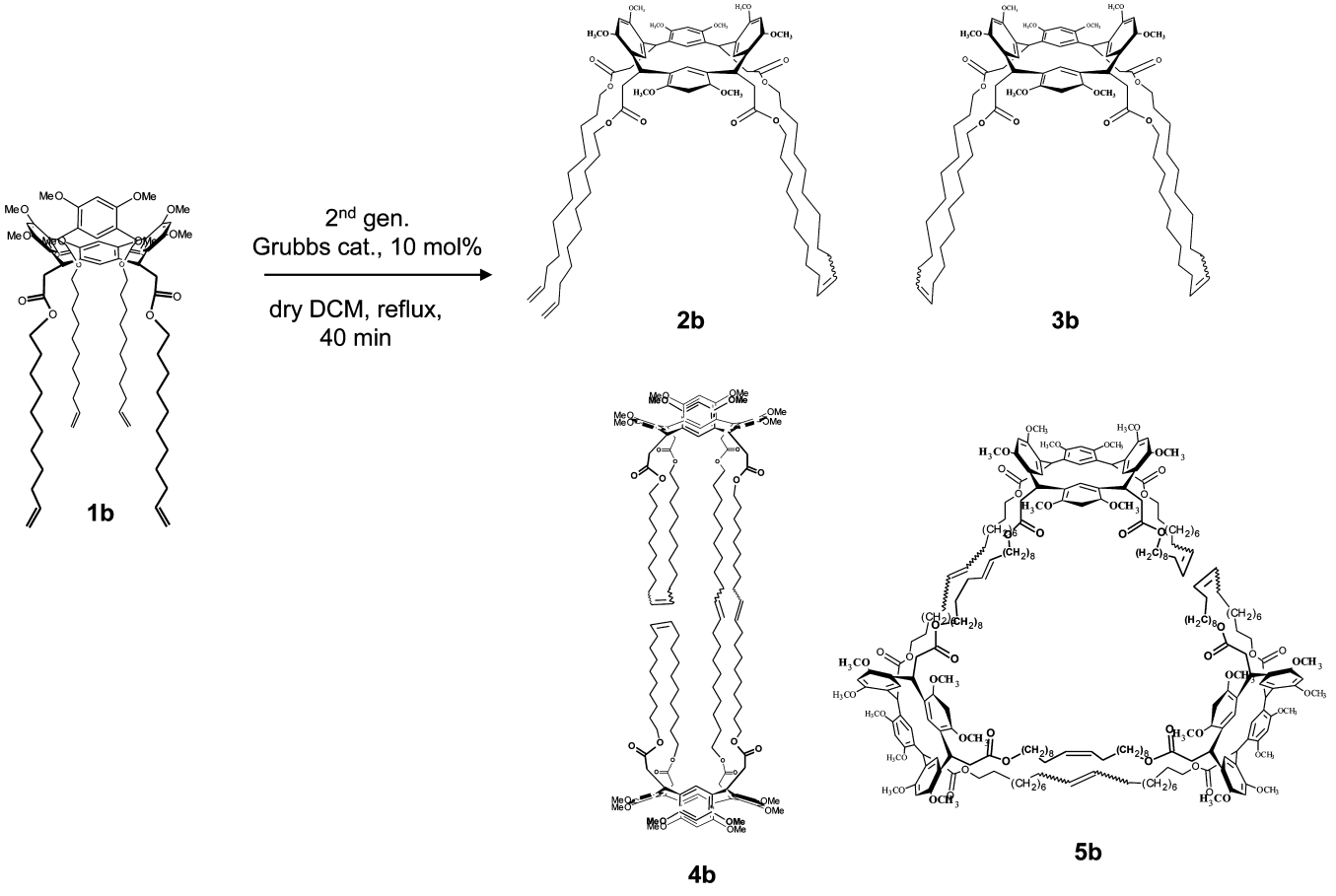

dx.doi.org/10.1021/jo502056v | J. Org. Chem. 2014, 79, 11051−11060

For the sake of comparison, the reaction parameters applied to resorc[4]arene **1b**, i.e., substrate concentration 3×10^{-3} M in DCM, second-generation Grubbs catalyst at 10 mol %, reflux temperature, were the same as used for the chair stereoisomer and had been optimized previously.[10]

The crude reaction mixture obtained under these conditions was treated with a metal scavenger (QuadraSil AP) to remove residual ruthenium by filtration and purified by silica-gel chromatography with an eluting mixture of increasing polarity (Experimental Section). The following products (Scheme 1) were isolated in order **2b** (yellow solid, 15% yield), **3b** (white solid, 50% yield), **4b** (white solid, 9% yield), and **5b** (white solid, 5% yield). The structures of compounds **2b**−**5b** were unambiguously confirmed through NMR spectroscopy (Tables 2−5 in the Experimental Section) and by electrospray ionization high-resolution mass spectrometry (ESI-HRMS). It is worth noting that undecenyl resorc[4]arene **1b** did not give any detectable polymer by olefin metathesis, whereas, at the same substrate concentration, the chair stereoisomer **1a** underwent an ADMET-like polymerization to furnish, despite unfavorable conditions, an insoluble oligomer product.[10] Evidently, the crowded arrangement of the cone conformation relative to those of the other conformations prevents the occurrence of such a reaction.

Structures of the Products Obtained by Olefin Metathesis. The ^{1}H and ^{13}C NMR spectral data of undecenyl resorc[4]arene **1b** have been reported previously.[10] The presence of single signals for equivalent aromatic and methoxyl protons and carbons suggested that the molecule assumes a cone conformation with C_{4v} symmetry in solution. All NOESY cross peaks have negative NOE values, indicating that the system is in a fast tumbling-motion regime, as expected for a conformation created by the equilibrium between two flattened-cone forms.[11]

Basket Resorc[4]arene 3b. Comparison of the NMR spectral data of **3b**, the most abundant product (50% yield), with those of the starting material resorc[4]arene **1b** exhibited the following points (Table 2 in the Experimental Section). Proton and carbon signals for the terminal methylene of **1b** are no longer present, whereas the signal for an olefin methine is still linked (as shown by TOCSY spectra) with the methylene groups of the chain but is high-field shifted. These findings confirm the occurrence of a RCM reaction, i.e., the formation of a double bond between two side chains with the elimination of one molecule of ethylene. Accordingly, the sodium adduct $[M + Na]^+$ in the ESI mass spectrum of **3b** was found at m/z 1407.84756, which is 56 amu ($2 \times C_2H_4$) less than the corresponding $[M + Na]^+$ peak of **1b** (m/z 1463.91035).[10] These findings fix the molecular weight of **3b** at about 1385 Da with a molecular formula of $C_{84}H_{120}O_{16}$, requiring two intramolecular bridges by two almost-contemporary RCM reactions. A second issue that emerged by comparison of the NMR spectra of compounds **3b** and **1b** is that the number of signals for the aromatic and methoxyl protons is, in the case of **3b**, basically doubled (vide infra), revealing a loss of symmetry of the upper rim. The distribution pattern of the signals, particularly the high-field resonances for the equivalent H25/H27 aromatic protons (A/C rings) and for the methoxyl groups (B/D rings), requires that the aromatic rings are alternatively quasiperpendicular; the B/D rings are face to face and the A/C rings lie almost in the same plane identified by the four bridge methines. NOESY spectra confirmed the spatial correlations between these protons and the internal aromatic protons (namely, H25/H27 and H26/H28), whereas strong positive cross peaks between H25/H27 and H26/H28 signals together with the absence of interaction peaks between external H5/H17 and H11/H23 aromatic protons supported a rigidified boat conformation with an all-cis configuration of the bridge chains.[11] We previously attributed such a conformation, also called a flattened cone, to a bridged resorcarene in which the insertion of two polymethyene bridges led to the formation of a cavity-shaped architecture resembling a basket.[12] The ^{1}H and ^{13}C NMR spectra of **3b**, however, are complicated by the presence of satellite signals; the resonance at $\delta = 5.31$ (br t, J = 4 Hz) for the disubstituted ═CH methine is flanked by a minor signal of the same nature (br t, J = 5 Hz) at $\delta = 5.33$. The two peaks in an approximate integrated ratio of 3:1 were correlated by TOCSY data to methylene signals at $\delta = 1.95$ and $\delta = 1.92$, the corresponding carbon resonances of which (by HSQC) appear at quite different values (δ = 32.6 and 28.9, respectively). The two peaks were thus assigned to E and Z olefinic protons, respectively, in agreement with the major shielding of the α-CH_2 in the Z configuration. Moreover, the high-field signal (δ = 5.31 ppm) showed a strong spatial correlation (by NOESY) with the protons of both α- and β-methylene groups, whereas the minor signal (at δ = 5.33 ppm) was NOE-correlated only to the protons of the geminal methylene nucleus, as expected for E and Z olefinic protons, respectively. With regard to the two different geometries of the double bond, three possible arrangements of the whole molecule can be envisaged: trans/trans, trans/cis, and cis/cis. The overall 3:1 ratio between the trans and cis signals indicates that the trans/trans, trans/cis, and cis/cis forms are in a ratio of 9:6:1, respectively. As a consequence, not only affected are the signals of the α-CH_2, but also affected are those of the whole ^{1}H NMR spectrum. Although the signals of the remaining methylene groups of the aliphatic chains cannot be distinguished, the chemical shifts of the singlets corresponding to the aromatic and methoxyl protons depend on three possible arrangements of the whole molecule. As a result, minor satellite peaks flank the major signals, attributed to the trans/trans form. Tentative assignments of all proton resonances of **3b**, taking into consideration the superimposition of some signals, are summarized in Table 2.

Catalytic hydrogenation (10% Pd/C) of **3b** afforded unique tetrahydrobasket **3br**, which showed the expected $[M + Na]^+$ peak at m/z 1411.87772 and clean signals without satellite peaks in the ^{1}H and ^{13}C NMR spectra (Supporting Information). The reduction reaction influenced the chemical shifts of the aromatic protons, which maintained, however, the distribution pattern (H25/H27, H11/H23, H5/H17, H26/H28) typical of a flattened cone conformation.

Hemibasket Resorc[4]arene 2b. In the ^{1}H and ^{13}C NMR spectra of the second product **2b** (15% yield), the signal for a disubstituted double bond (at $\delta = 5.32$ ppm, as in **3b**) and that for the AMN system of the vinylidene group (at δ = 5.82, 4.99, and 4.93 ppm, respectively, as in parent resorc[4]arene **1b**) were found (Table 3 in the Experimental Section). These findings and the signal from the sodium adduct $[M + Na]^+$ in the ESI mass spectrum at m/z 1435.87745 suggest that only one ring closure occurred between two side chains, leaving the remaining two side chains free. The complicated distribution pattern of the signals in the ^{1}H NMR spectrum of **2b**, i.e., mainly doubling for aromatic protons and methoxyl groups, was attributed to the presence of two forms in equilibrium, originated by the loss of freedom of the aromatic ring B (Figure

dx.doi.org/10.1021/jo502056v | J. Org. Chem. 2014, 79, 11051−11060

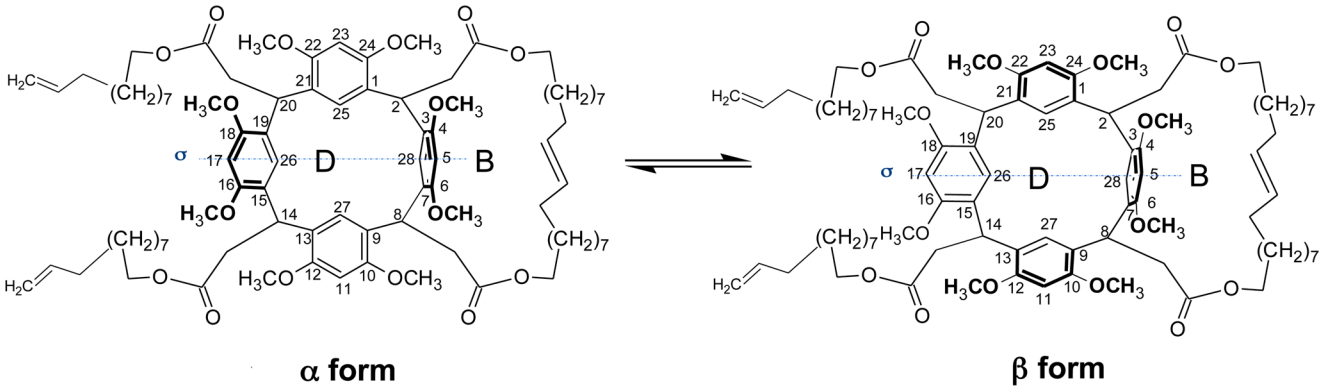

Figure 1. Forms in equilibrium for hemibasket **2b** in solution.

1) connected to the new bridge chain. The two forms are depending on the free oscillation of ring D, which can be approximately parallel (α) or perpendicular (β) to opposite ring B. The α-form maintains the arrangement of a flattened version of the original cone conformation, i.e., that of starting compound **1b**, whereas the β-form assumes the conformation of a chairlike partially flattened cone.

The ^{1}H NMR spectral data of the two conformations of **2b** are expected to be quite similar,[11] and a nontentative assignment is possible only for proton H26, which is subject to different shielding effects from aromatic ring B in the α and β forms. The presence in the proton spectrum of minor signals in the regions of the aromatic rim was again attributed to the α and β forms of the cis isomer, in a ratio of 1:2 with the trans isomer, as confirmed by integration of the signals at δ = 5.34 (br t, J = 4 Hz) and δ = 5.32 (br t, J = 3 Hz), respectively. Compound **2b** is obviously the intermediate precursor of basket **3b**, and in this view, it can be designated as a hemibasket.

Dimer 4b. With regard to compound **4b**, the first of two more minor and more polar products (9% yield), the ^{1}H and ^{13}C NMR spectral data (Table 4 in the Experimental Section) were very similar to those of basket derivative **3b**. Again, the signals for the terminal methylene in starting material **1b** were replaced by those for two disubstituted trans double bonds. In fact, the two =CH resonances were linked to methylene signals at δ = 32.2 and 32.7, which requires both to be in the α position relative to a trans double bond. In the ^{1}H NMR spectrum, the signals for a cis olefin could not be distinguished from the two main values (δ = 5.36 and 5.32), whereas in the ^{13}C NMR spectrum, the resonances at δ = 130.8 and 130.1 were flanked by two smaller partners (visually 30%) at δ = 129.7 and 129.6. Therefore, we hypothesized the presence of two different types of chains, the first involving a sequence of signals for =CH, α-CH_2, and β-CH_2 comparable to those of **3b** and the second with slightly different values for the above groups, both ending in a series of methylenes (γ to ω) giving indistinguishable signals. The changes in the second chain were attributed to the formation of two intermolecular double bonds between two side chains of two molecules, whereas the other two original intramolecular double bonds remained unchanged, resulting in a closed dimer with structure **4b** (Scheme 1). Two diagnostic peaks at m/z 2792.69337 and 1407.84371 in the ESI mass spectrum, which were attributed to $[M + Na]^+$ and $[M + 2Na]^{2+}$ sodium adducts, respectively, revealed for dimer **4b** a molecular weight of 2769.7 Da (2 times that of **3b**) and a molecular formula of $C_{168}H_{240}O_{32}$. Both the diagnostic peaks originated serial losses of CH_2 (14 and 7 amu, respectively) as expected for compounds endowed with a long hydrocarbon chain. The distribution pattern of the signals for aromatic and methoxyl protons was again in agreement with a flattened cone arrangement of the two aromatic rims. However, weakly negative NOESY peaks between H25/H27 and H26/H28 suggested the interconversion between two flattened cone α and β forms, where two opposite aromatic rings, e.g., A/C, are alternatively vertical or planar, respectively.[11] Moreover, negative NOE peaks between H5/H17 and the corresponding methoxyl protons, as well as positive NOE peaks between H11/H23 and the corresponding methoxyl protons, require that planar and vertical aromatic rings have different mobility. Additionally, the α-CH_2 signal shows a cross peak with the H26/H28 resonance in both NOESY and ROESY spectra, but it could be correlated to the H25/H26 protons only in the ROESY experiment. These findings suggest that the oscillations of the two flattened-cone α and β forms undergo a slow down as a consequence of the presence of two different side chains and will have longer lifetimes than the NMR acquisition time. Consequently, the signals from both conformations will be registered as it happens for the quite similar hemibasket compound **2b**.

Indeed, the ^{1}H NMR spectrum of **4b** is characterized by the presence of multiple or broadened (br) signals for aromatic protons and methoxyl groups, whereas the appearance of the aliphatic methine at δ = 4.94 as a triplet (with J = 7.5 Hz) instead of a double doublet (with J = 7 and 8 Hz) testifies to the relative freedom of **4b** as compared to that of **3b** caused by the formation of a larger macrocycle.

Trimer 5b. The NMR spectral data of the second polar product **5b** (5% yield) are almost coincident with those of **4b** (Table 5 in Experimental Section). Two different trans CH= moieties are still present, suggesting the presence of both inter- and intramolecular double bonds, whereas the multiplicity of the aliphatic methine carbons (t, J = 7 Hz) accounts for a mobility of **5b** comparable to that of **4b**. Conversely, the signals for the aromatic rim appear to be multiplied and coalesced in some cases. The ESI mass spectrum of **5b** showed a diagnostic peak at m/z 2100.76621, which was assigned to the doubly charged $[M + 2Na]^{2+}$ sodium adduct. A trimeric structure (as compared the monomeric structure of **3b**), a molecular weight of about 4154 Da, and a corresponding molecular formula of $C_{252}H_{360}O_{48}$ were thus assigned to compound **5b**.

Plausible Mechanism of the Olefin Metathesis Reaction. During the synthesis of basket **3b** from undecenyl resorc[4]arene **1b**, the starting material passes through the

dx.doi.org/10.1021/jo502056v | J. Org. Chem. 2014, 79, 11051−11060

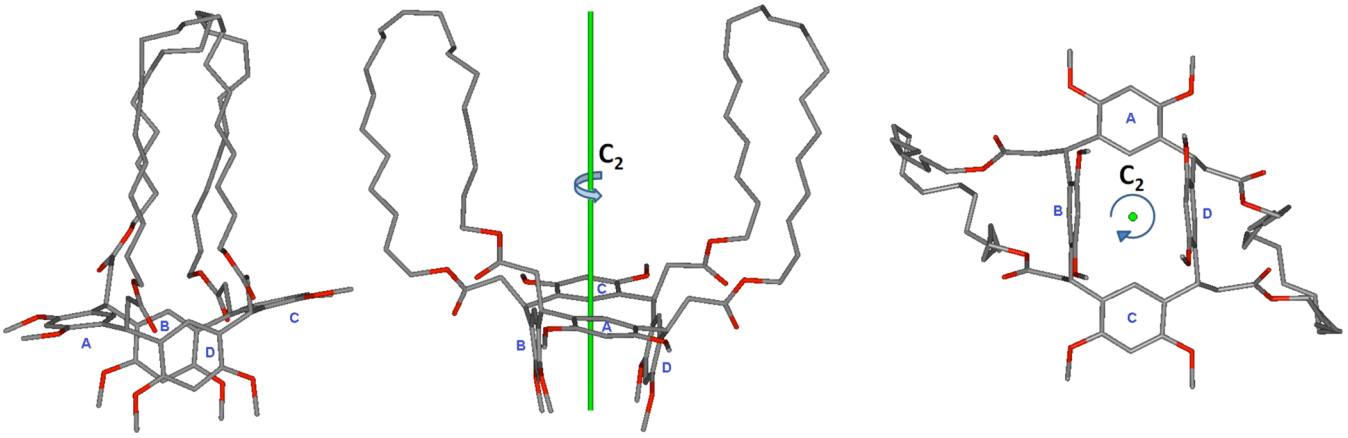

Figure 2. X-ray structure of basket resorc[4]arene **3b** showing the flattened cone conformation adopted by the macrocycle. Carbon, gray; oxygen, red. Hydrogen atoms are omitted for clarity.

formation of hemibasket **2b**, which occurs by two almost-contemporary RCM reactions driven by the loss of two molecules of ethylene as we have already proposed.[10] Notably, although we did not isolate the hemifunctionalized intermediate in the case of the chair stereoisomer **1a**, now we can confirm the proposed reaction mechanism.

The attribution of homodimer and homotrimer structures to **4b** and **5b**, respectively, and the central importance of basket derivative **3b** in the overall metathesis reaction were confirmed by submitting a pure sample of **3b** to the same olefin metathesis conditions (catalyst loading, temperature, and time) as those used for **1b** (Experimental Section). As a result, compounds **4b** and **5b** were again obtained in 7 and 10% yields, respectively, and around 23% of unreacted starting **3b** was recovered. These results exclude the possibility that the central ring of the two **4b** and **5b** compounds could have originated from two intermolecular cross-metathesis (CM) reactions, because the formation of the macroring would require the opening of two smaller rings and a novel closure of the largest one. Additionally, we have already shown that the intermolecular closure between chains of different molecules could likely start via an ADMET-like polymerization.[10]

X-ray Diffraction Analysis of Basket Resorc[4]arene 3b. The molecular structure of basket **3b** at the solid state as resolved by X-ray diffraction analysis is illustrated in Figure 2. Taking as a reference the weighed least-squares plane (R_plane) passing through the four bridging carbon atoms of the macrocycle, the measured dihedral angles δ[13] (collected in Table 1) show that the A and C aromatic rings are almost coplanar (8.46° below and 9.68° above, respectively) with the R_plane, whereas B and D are almost orthogonal to it (82.25° and 80.05°, respectively). Following a procedure already reported,[14] the molecular conformation of the macrocycle was given by the conformational parameters ϕ and χ, which account without ambiguity for the reciprocal orientations between adjacent aromatic rings (Table 1). The sequence of signs (+/−,+/−,+/−,+/−) of the measured values of ϕ and χ suggested a flattened cone conformation for basket **3b**. As shown in Figure 2, the two ester bridging loops protruding above the resorcarene basket leave a large intramolecular space available for inclusion of other chemical species. Because in the X-ray detected structure the minimum interatomic distances between the carbon atoms of two opposite bridges are ∼10 Å, it can be expected that, under suitable conformational changes, the hydrocarbon arms easily adapt to molecular guests with sizes around 10 Å, resembling the movement of a molecular gripper.[15]

As a result of the above-described structure, basket resorc[4]arene **3b** yields a peculiar self-assembly at the solid state represented by the supramolecular architectures shown in Figure 3 and Figure S1. This "secondary structure" is built up in a way that fills the intramolecular space between two hydrocarbon loops of each **3b** molecule with one ester handle of an adjacent molecule (the bridge chain hereafter denoted as the incapsulated arm), which is turned 180° along the axis passing through the flattened aromatic rings. The multi-

Table 1. Dihedral Angles (δ) and Conformational Parameters (ϕ and χ) for Basket 3b

rings[a]	δ (deg)[b]	rings	ϕ (deg)[b]	χ (deg)[b]
R_plane A	171.54(5)	A–D	150.2(2)	−76.7(2)
R_plane B	82.25(5)	D–C	66.6(2)	−157.7(3)
R_plane C	189.68(5)	C–B	165.6(3)	−89.1(2)
R_plane D	80.05(4)	B–A	59.9(2)	−132.9(2)

[a]R_plane is the weighed least-squares plane passing through the four bridging carbon atoms of the macrocycle. [b]Estimated standard deviations (ESD) are reported in parentheses.

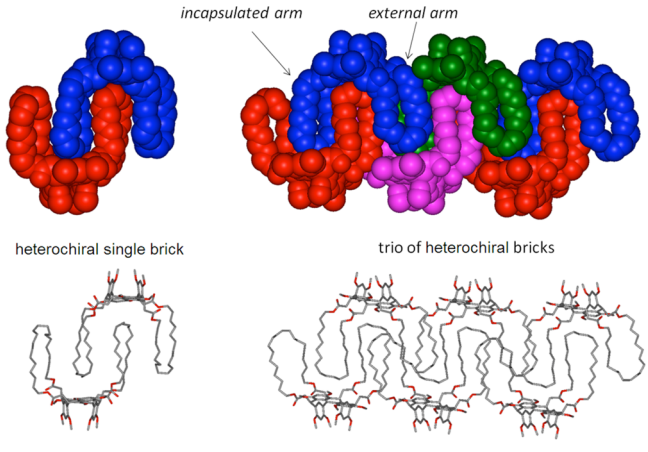

Figure 3. CPK (top) and stick views (bottom) of basket resorc[4]-arene **3b** in crystal lattice. Supramolecular dimer (left) and zigzag 1D ribbon (right) as a trio of heterochiral dimers.

dx.doi.org/10.1021/jo502056v | J. Org. Chem. 2014, 79, 11051−11060

assembly of such a supramolecular dimer that represents the brick unit of the resolved crystal lattice significantly differs from that which is observed for a similar basket resorc[4]arene with much shorter and saturated bridge chains.[12] In the case of **3b**, because of a peculiar inherently dissymmetric conformation assumed by each molecule in the crystal lattice (for the presence of a C_2 axis of symmetry normal to the R_plane of a single molecule, see Figure 2), the assembly produces zigzag 1D ribbons, such as those depicted in Figure S1. In the supramolecular arrangement, **3b** is induced to assume an inherent chirality with two heterochiral dimeric brick units overlooking one another sideways, allowing contact between the incapsulated arm of one unit with the unencapsulated hydrocarbon loop of the other. The driving forces for such a packing arrangement seem to be (i) the complementary zigzag alternation of the dipole moments associated with the single molecules (the calculated dipole moment being 3.046 D) and (ii) the effective maximization of favorable interactions that strongly minimizes the empty spaces between the molecular units.

In addition to the above-described supramolecular zigzag 1D ribbons (which display a polar surface in both their up and down sides), a peculiar "tertiary structure" was also detected in the crystal lattice for basket resorc[4]arene **3b**, in which a lamellar-type crystalline organization is built up by the interdigitation of the methoxyl groups of one ribbon between those of the first adjacent ribbon. The layers are extended along crystallographic axis (*b*) and bisect crystallographic plane (*ac*), as illustrated in Figure S1. On the other hand, when the crystal lattice is viewed orthogonally to crystallographic axis (*b*), i.e., orthogonally to the plane of Figure S1, it shows a multilayered structure containing intercalated hydrophilic and hydrophobic layers (ca. 9 and 10 Å thick, respectively).

Overall, X-ray diffraction analysis showed that basket **3b** has a strong propensity to self-assemble, which prompted us to investigate more deeply the hydrophilic−hydrophobic balance of the molecule. Such information, in fact, could be helpful in the selection of suitable guests capable of interacting with resorc[4]arene **3b** within its basketlike cavity.

Evaluation of the Hydrophilic−Hydrophobic Balance of Basket 3b. Following a procedure already reported,[16] we monitored the self-assembly of basket **3b** in solution by UV−visible spectroscopy. With regard to the choice of the proper solvent system, preliminary analysis showed that basket **3b** is fairly soluble in medium-polarity solvents (e.g., THF, chloroform, and ethyl acetate), sparingly soluble in both apolar (e.g., *n*-hexane) and polar (e.g., acetonitrile and methanol) solvents, and nearly insoluble in water. For this reason, we decided to employ a binary THF/water system that was expected to allow the aggregation of basket **3b** within a proper composition range. For this purpose, THF/water solutions of basket **3b** at a constant concentration of 8.8×10^{-4} M were prepared by adding increasing amounts of water to a stock THF solution (for details, see the Experimental Section). The aggregation process of **3b** was then monitored by recording UV−vis absorbance spectra of the above-mentioned solutions over a wavelength range of 200−800 nm as a function of increasing polarity. Changes induced by the self-assembly process are clearly visible in the UV−vis spectra collected in Figure 4. UV−vis profiles of solutions with a THF concentration greater than 52% (v/v, red) display two quite sharp absorption bands at 228.5 and 284.5 nm and a minimum of absorption at 261.0 nm that are indistinguishable from those obtained in pure THF and

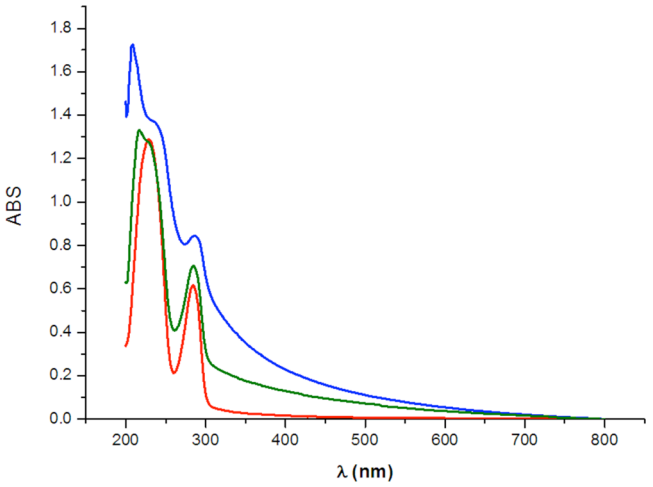

Figure 4. UV−visible spectra of basket resorc[4]arene **3b** (8.8×10^{-4} M) in different THF/water solvent systems: THF/water (v/v) > 52%, red; THF/water (v/v) < 40%, blue; 40% < THF/water < 52%, green.

therefore indicate that basket **3b** is present as a monomer. In contrast, when THF concentration was less than 40% (v/v, blue), a wide broadening of all the absorption bands was detected as well as an increasing absorption drift at the lowest wavelength values and the appearance of a shoulder at 232 nm (blue). Notably, such an absorption trend was invariant to any further decrease of THF concentration in the solvent system. This behavior is typical in systems that have achieved complete substrate aggregation, which is responsible for the generation of colloidal systems that trigger light scattering phenomena. Any intermediate compositions of THF/water solutions, i.e., those featuring a THF concentration ranging from 40 to 52%, v/v, yielded an intermediate absorption trend (green) for basket **3b**.

For the calculation of a properly normalized difference in absorbance (ΔABS_{norm}), defined as in eq 1, the maximum and minimum absorption bands of 284.5 and 261.0 nm, respectively, were selected.

$$\Delta ABS_{(261.0-284.5)norm} = \frac{(\Delta ABS_{curr} - \Delta ABS_{aggr})}{(\Delta ABS_{mono} - \Delta ABS_{aggr})} \times 100 \quad (1)$$

In eq 1, the subscripts "aggr" and "mono" refer to the absolute UV absorbance differences that **3b** displays between 261.0 and 284.5 nm in THF/water mixtures at which it is certainly in completely aggregated or momomeric form, respectively, and the subscript "curr" denotes the same type of absorbance difference measured in the generic THF/water mixture currently analyzed.

By plotting the $\Delta ABS_{(261.0-284.5)norm}$ values obtained according to eq 1 as a function of the Hildebrand polarity index (δ_H)[16] of the THF/water solvent systems, a typical sigmoidal aggregation curve was obtained for basket **3b** (Figure 5 and Table 1S). Regression analysis of the sigmoidal plot to fit the data points was performed according to eq 2, yielding an already described parameter, namely, the aggregation polarity index (API),[16] that proved useful to predict the propensity of a species to self-assembly at a given substrate concentration[17] because it directly reflects in a quantitative fashion the hydrophilic/hydrophobic nature of the molecule.

$$\Delta ABS_{(261.0-284.5)norm} = 100/\{1 + 10^{[(\delta_H - API/a)]}\} \quad (2)$$

dx.doi.org/10.1021/jo502056v | J. Org. Chem. 2014, 79, 11051−11060

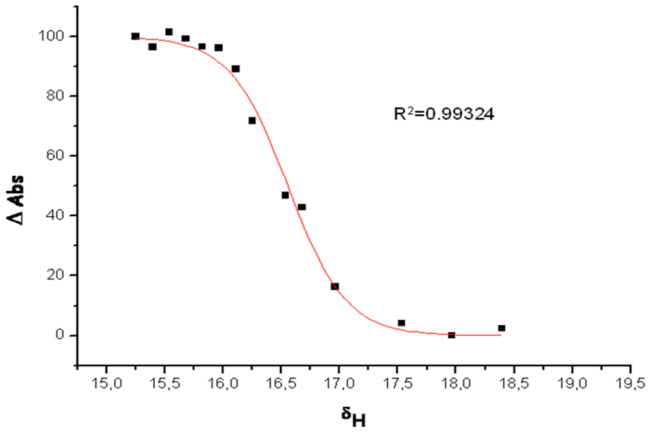

Figure 5. Sigmoidal aggregation profile of basket resorc[4]arene **3b** as obtained in THF/water solvent system. Regression analysis to fit the experimental data was performed according to eq 2.

Indeed, API is the solvent polarity, expressed as the δ_H index, that corresponds to a 50% variation of $\Delta ABS_{(261.0-284.5)norm}$, denoting that 50% self-aggregation was achieved. The variable a in eq 2 is a further tunable parameter that can be used to take into account the gradient of variation of $\Delta ABS_{(261.0-284.5)norm}$ as a function of the δ_H index, yielding the δ_H values at which the aggregation starts (δ_H^{start}) and ends (δ_H^{end}) with respect to API ($\delta_H^{start} \cong API - a \pm 0.1$; $\delta_H^{end} \cong API + a \pm 0.1$). For basket **3b**, an API value of 16.56 ± 0.02 $(kcal\ dm^{-3})^{1/2}$ was calculated, which corresponds to a solvent composition where THF/water = 48:52 (v/v) (with a = 0.57).

This means that the aggregation of **3b** starts approximately when the THF/water solvent composition yields δ_H = 16.0, i.e., THF/water = 52:48, v/v, and stops when δ_H = 17.1, i.e., THF/water = 44:56, v/v. Notably, because δ_H is also correlated to the cohesion energy of the solvent, the higher the value of API, the more energy is required for the formation of cavities within the solvent where the substrate units may be hosted (in both the monomer form and supramolecular aggregate forms). Therefore, the not particularly high API value found for basket **3b** suggests that quite intense solvophobic interactions begin to form between molecules in aggregation at a water concentration of barely 48% (v/v). In other words, the calculation of API allowed us to confirm that in basket **3b** the hydrophobic nature largely overcomes the hydrophilic one.

Solvophobic interactions can be quantified by calculating the cavitation Gibbs free-energy change ($\Delta\Delta G_{cav}$), which is the change of free energy occurring for the insertion of a cavity into a solvent, in response to the change of solvent composition before and after the self-assembly phenomena in a given solute. Such a value can be calculated by eq 3, as already reported.[16]

$$\Delta\Delta G_{cav} = (\kappa_2\gamma_2 - \kappa_1\gamma_1)A \quad (3)$$

where $\kappa_2\gamma_2$ and $\kappa_1\gamma_1$ are the corrected surface tensions of the given solvent systems corresponding to the beginning and the end of solute aggregation, respectively, and A is the molecular surface of the same species in its unaggregated form. Thus, knowing the relationship between δ_H and the corrected surface tension $\kappa\gamma$ for the THF/water solvent systems,[18] we calculated the difference $\kappa_2\gamma_2 - \kappa_1\gamma_1 = 5.13 \times 10^{-7}$ kcal/m^2. Molecular mechanics calculations based on the MMFF force field (Experimental Section for details) yielded the missing value A (9.32×10^6 m^2 mol^{-1}). To compute $\Delta\Delta G_{cav}$ for basket **3b**, we simply substituted the above values in eq 3 and found that the cavitation Gibbs free-energy change associated with the self-assembly of macrocycle **3b** is 4.78 kcal mol^{-1}. Notably, unlike API, $\Delta\Delta G_{cav}$ is a concentration-independent function, as previously demonstrated.[16]

A final physical parameter involved in the self-assembly phenomena is the decrease of the molecular surface A that a given solute exposes to the solvent upon aggregation to minimize the free energy (%ΔA). The value for basket **3b**, calculated according to eq 4, was 5.90%.

$$\%\Delta A = |(\kappa_1\gamma_1/\kappa_2\gamma_2 - 1)| \times 100 \quad (4)$$

We demonstrated that, taken together, API, $\Delta\Delta G_{cav}$ and %ΔA proved useful descriptors to monitor the propensity of basket **3b** to self-assembly in THF/water solutions. With regard to the hydrophilic−hydrophobic ratio, basket **3b** showed a trend comparable to that previously observed for some amphiphilic C_{60} fullerene derivatives (FDs) in the same solvent system[16] whose structures are shown in Table 2S. By inspection of the data collected in Table 2S, it may be clearly seen that according to all the above three parameters the hydrophilic/hydrophobic balance of **3b** ranks after that of **FD3** and before that of **FD4**, being more similar to that of **FD3** (API = 16.0 $(kcal\ dm^{-3})^{1/2}$, $\Delta\Delta G_{cav}$ = 1.69 kcal mol^{-1}, %ΔA = 3.22), which is a fulleropyrrolidine functionalized with a hydrophilic pendant (Figure 6). The comparison is also supported by the close

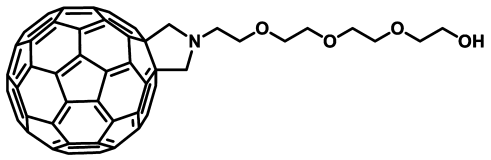

Figure 6. Structure of a C_{60} fulleropyrrolidine functionalized with a hydrophilic pendant[16] that showed an hydrophilic−hydrophobic ratio quite similar to that of basket **3b**.

agreement of $\Delta\Delta G_{cav}$ and %ΔA values for basket **3b** with the relevant data for **FD1**−**FD5** (Figure S3). Such similarity suggests that if the C_{60} fullerene sphere was accommodated within the hydrophobic cage of resorc[4]arene **3b** (an interaction conceivable in terms of both reciprocal size and hydrophobicity), the resulting supramolecular adduct would display a hydrophilic/hydrophobic balance similar to that shown by fulleropyrrolidine **FD3**. In other words, the fullerene sphere could be made amphiphilic in the whole by host−guest interaction. A similar trend could also be expected in polar solvents with any further apolar guests endowed with the suitable size. We could even imagine tuning the amphiphilic properties of the supramolecular species obtained by chemically modifying the polar surface of basket **3b**. Such reversible manipulation of the chemical properties of fullerenes could have an interesting impact on their wide field of applications, i.e., materials technology, microelectronics, biology, and medicinal chemistry.[19]

CONCLUSIONS

We carried out an olefin metathesis reaction on a resorc[4]-arene featuring 11 carbon side chains ending with a vinylidene group, fixed in the cone conformation. The basic idea was to compare the results previously obtained on the same substrate but featuring a different arrangement of the four undecenyl side chains (namely, a chair conformation). Notably, the cone stereoisomer did not give any detectable polymer by olefin

dx.doi.org/10.1021/jo502056v | J. Org. Chem. 2014, 79, 11051−11060

metathesis, whereas at the same substrate concentration, the chair stereoisomer underwent an ADMET-like polymerization to furnish, despite unfavorable conditions, an insoluble oligomer product. Another notable result was the conformational change (absent in the chair conformation) induced by the ring closure that yielded a double-spanned resorc[4]arene endowed with novel properties. This compound showed a strong propensity to self-assembly in the solid state as a supramolecular trio of heterochiral dimers. Therefore, we developed a set of physical descriptors that together allowed us to calculate the hydrophilic−hydrophobic balance of the macrocycle in solution. On the basis of the results obtained, we can reasonably expect that such a "baseball glove" molecule is suitable for combination with various cocrystallizing species to yield rationally designed noncovalent molecular assemblies in the solid state. The next step of the study will be the docking different guests, i.e., the fullerene family, within the hydrophobic cavity of the basket and the investigation of complexation phenomena in solution.

EXPERIMENTAL SECTION

General Procedures and Materials. All manipulations were performed using a combination of glovebox and high vacuum under a nitrogen atmosphere. HPLC grade solvents were dried and degassed by standard procedures. Second-generation Grubbs catalyst and QuadraSil AP silica gel were purchased from a chemical supplier.

Olefin Metathesis Reaction on Undecenyl Resorc[4]arene 1b. Resorc[4]arene ω-undecenyl ester **1b**, obtained as previously described,[10] (0.25 g, 0.17 mmol) was dissolved in dry DCM (57 mL) to reach a final substrate concentration of 3.0×10^{-3} M. The solution was held at reflux temperature and then exposed to a solution of catalyst [$(H_2IMes)(PCy_3)(Cl)_2Ru{=}CHPh$)] (0.015 g, 0.017 mmol, 10 mol %) in dry DCM (3 mL), previously prepared in the glovebox. The reaction mixture was kept at reflux under stirring and a nitrogen atmosphere for 40 min and then treated with QuadraSil AP metal scavenger (aminopropyl silica gel, 4 g). After 5 min, the mixture was cooled to room temperature and left under stirring overnight. After filtration and evaporation, the residue was suspended in DCM and applied to a silica-gel column to give compounds **2b** (36 mg; 15%) and **3b** (120 mg; 50%) with DCM/ethyl acetate = 91:9 and compound **4b** (21.5 mg; 9%) and compound **5b** (12 mg; 5%) with chloroform/methanol = 99:1.

Compound ***3b***. White solid, mp 175−176 °C, 120 mg, 0.087 mmol (50% yield). ^{1}H and ^{13}C NMR signals are given in Table 2. ESI-HRMS (positive) $C_{84}H_{120}O_{16}Na$ requires 1407.84686 (monoisotopic mass), *m*/*z* found 1407.84756 ($[M + Na]^+$). FT-IR (KBr) 2921, 2850, 1728, 1583, 1506, 1301, 1201 cm^{-1}.

Compound ***2b***. Yellow solid, mp 123−124 °C, 36 mg, 0.025 mmol (15% yield). ^{1}H and ^{13}C NMR signals are given in Table 3. ESI-HRMS (positive) $C_{86}H_{124}O_{16}Na$ requires 1435.87871 (monoisotopic mass), *m*/*z* found 1435.87745 ($[M + Na]^+$). FT-IR (KBr) 2921, 2850, 1728, 1583, 1506, 1301, 1201 cm^{-1}.

Compound ***4b***. White solid, mp 144−145 °C, 21.5 mg, 0.008 mmol (9% yield). ^{1}H and ^{13}C NMR signals are given in Table 4. ESI-HRMS (positive) $C_{168}H_{240}O_{32}Na$ requires 2792.70450 (monoisotopic mass),

Table 2. ^{1}H NMR and ^{13}C NMR Chemical Shifts (δ, ppm) for Basket Resorc[4]arene 3b[a]

carbon	^{1}H	^{13}C
C=O		172.5
C_{Ar}–O		156.4
		155.7
CH=[b]	5.31 br t (4)	130.7
CH_i (25,27)	6.12 br s	126.2
CH_i (26,28)	6.88 br s	125.4
C_{Ar}–C		125.0
		123.2
CH_e (5,17)	6.16 br s	97.4
CH_e (11,23)	6.42 br s	95.2
OCH_2	3.99 dt (10.7, 6.8)	64.3
	3.90 dt (10.7, 6.8)	
OMe	3.82 s	55.9
	3.42 s	55.8
CH_2–(CO)	2.78 dd (15.5, 8)	39.1
	2.76 dd (15.5, 7)	
CH	4.94 dd (8, 7)	33.0
CH_2–(CH=)[b]	2.02 m	32.1
CH_2–(CH_2–CH=)	1.33 m	29.3
CH_2–(CH_2O)	1.53 br m	28.6
CH_2 × 5	1.23 br m	29.5
		29.1
		29.0
		28.1
		26.0

[a]NMR conditions: 600 MHz (^{1}H) and 100 MHz (^{13}C), $CDCl_3$, *T* = 300 K. Coupling constants *J* (Hz) are given in parentheses. [b]Only signals assigned to the predominant stereoisomer (namely, *E*) are reported.

Table 3. ^{1}H NMR and ^{13}C NMR Chemical Shifts (δ, ppm) for Hemibasket Resorc[4]arene 2b[a]

carbon	^{1}H	^{13}C
C=O		172.5, 172.4
C_{Ar}–O		156.1, 156.0
		155.7, 155.5
CH=(CH_2)	5.82 ddt (17, 10, 6.5)	139.2
CH=(CH)[b]	5.32 br t (3)	130.7
CH_i (25,27)	6.31, 6.17	126.4, 126.1, 125.5
CH_i (26,28)	6.84, 6.71	
C_{Ar}–C		
$=CH_2$	4.99 br d (17)	114.1
	4.93 br d (10)	
CH_e (5,17)	6.22, 6.19	97.1, 97.0
CH_e (11,23)	6.46, 6.36	95.5, 95.8
OCH_2	3.97 dt (10.8, 6.5)	64.3
	3.95 t (7)	64.3
	3.91 m	
OMe	3.89, 3.72, 3.51, 3.48	55.9
CH_2–(CO)	2.83 d (7)	39.1
	2.82 m	
CH	4.95 m[c]	33.1, 32.9
CH_2–(CH=)	2.03 br q (6.5)	33.8, 32.1
	1.98 m	
CH_2–(CH_2–CH=)	1.36 m	29.0, 29.0
	1.33 m	
CH_2–(CH_2O)	1.52, 1.47 m	28.6, 28.6
CH_2 × 5	1.24 br m	29.6
		29.3
		29.2
		29.0
		26.0

[a]NMR conditions: 600 MHz (^{1}H) and 100 MHz (^{13}C), $CDCl_3$, *T* = 300 K. Coupling constants *J* (Hz) are given in parentheses. [b]Only signals assigned to the predominant stereoisomer (namely, *E*) are reported. [c]Tentative assignment due to superimposition of the $=CH_2$ signals.

dx.doi.org/10.1021/jo502056v | J. Org. Chem. 2014, 79, 11051−11060

Table 4. ^{1}H NMR and ^{13}C NMR Chemical Shifts (δ, ppm) for Dimer 4b[a]

carbon	^{1}H	^{13}C
C═O		172.5
C_{Ar}–O		156.4
		155.7
CH═[b]	5.32 m	130.8
	5.36 m	130.1
CH_i (25,27)	6.16 × 2, 6.14, 6.11 br s	126.2
CH_i (26,28)	6.94, 6.91, 6.90, 6.89 br s	125.4
C_{Ar}–C		125.1
		123.3
CH_e (5,17)	6.19 × 3, 6.18 br s	97.6
CH_e (11,23)	6.46, 6.41 × 3 br s	95.6
OCH_2	3.99 dd (11.5, 7)	64.5
	3.93 dd (11.5, 7)	
OMe	3.85, 3.83 × 3 br s	56.2
	3.45 × 3, 3.43 br s	55.9
CH_2–(CO)	2.83 br d (7)	39.2
CH	4.94 t (7.5)	33.1
CH_2–(CH═)[b]	1.98 m	32.7
	2.02 m	32.2
CH_2–(CH_2–CH═)	1.33 m	29.4
	1.31 m	
CH_2–(CH_2O)	1.53 br m	28.7
CH_2 × 5	1.24 br m	29.5
		29.2
		29.0
		28.2
		26.0

[a]NMR conditions: 600 MHz (^{1}H) and 100 MHz (^{13}C), $CDCl_3$, T = 300 K. Coupling constants J (Hz) are given in parentheses. [b]Only signals assigned to the predominant stereoisomer (namely, E) are reported.

Table 5. ^{1}H NMR and ^{13}C NMR Chemical Shifts (δ, ppm) for Trimer 5b[a]

carbon	^{1}H	^{13}C
C═O		172.4
C_{Ar}–O		156.3
		155.4
CH═[b]	5.32 m	130.7
	5.36 m	130.2
CH_i (25,27)	6.14 br s	126.1
CH_i (26,28)	6.87 br s	125.4
C_{Ar}–C		124.9
		123.2
CH_e (5,17)	6.17 br s	97.3
CH_e (11,23)	6.41 br s	95.3
OCH_2	3.96 m	64.2
	3.92 m	
OMe	3.82 br s	56.0
	3.41 br s	55.7
CH_2–(CO)	2.81 m	39.0
CH	4.95 t (7.5)	32.9
CH_2–(CH═)	1.94 m	32.5
	1.98 m	32.1
CH_2–(CH_2–CH═)	1.32 m	29.6
	1.30 m	
CH_2–(CH_2O)	1.50 m	28.5
CH_2 × 5	1.23 br m	29.6
		29.3
		29.0
		28.6
		26.7

[a]NMR conditions: 600 MHz (^{1}H) and 100 MHz (^{13}C), $CDCl_3$, T = 300 K. Coupling constants J (Hz) are given in parentheses. [b]Only signals assigned to the predominant stereoisomer (namely, E) are reported.

m/z found 2792.69337 ($[M + Na]^+$); $C_{168}H_{240}O_{32}Na_2$ requires 1407.84686 (monoisotopic mass), m/z found 1407.84371 ($[M + 2Na]^{2+}$). FT-IR (KBr) 2923, 2852, 1736, 1508, 1458, 1300, 1203 cm^{-1}.

*Compound **5b**.* White solid, mp 150–151 °C, 12 mg, 0.0029 mmol (5% yield). ^{1}H and ^{13}C NMR signals are given in Table 5. ESI-HRMS (positive) $C_{252}H_{360}O_{48}Na_2$ requires 2100.76230 (monoisotopic mass), m/z found 2100.76621 ($[M + 2Na]^{2+}$). FT-IR (KBr) 2923, 2852, 1736, 1508, 1458, 1300, 1203 cm^{-1}.

Catalytic Hydrogenation of Basket Resorc[4]arene 3b. After two vacuum/nitrogen cycles to replace the air atmosphere inside the reaction tube, compound **3b** (42 mg, 0.030 mmol) and 10% Pd/C (10 mg) in dry THF (5 mL) were vigorously stirred at room temperature under 1 atm of hydrogen for 24 h. The reaction mixture was filtered through a membrane filter (Millex-LH, 0.45 μm), and the filtrate was concentrated. Purification of the residue by silica-gel chromatography (DCM/ethyl acetate = 99:1→ 97:3) gave tetrahydrobasket **3br** (42 mg, 0.030 mmol, quantitative yield).

*Tetrahydrobasket Resorc[4]arene **3br**.* White solid, mp 172–173 °C, 42 mg, 0.030 mmol (quantitative yield). ^{1}H NMR (400 MHz, $CDCl_3$, 300 K) δ (ppm) 6.70 (s, CH_i26,28), 6.36 (s, CH_e5,17), 6.35 (s, CH_e11,23), 6.23 (s, CH_i25,27), 4.87 (t, J = 7 Hz, 4H, CH), 3.86 (m, 4H, OCH_2), 3.71 (s, 12H, OMe), 3.54 (s, 12H, OMe), 2.82 (d, J = 7 Hz, 4H, CH_2–CO), 1.54 (m, 8H, CH_2–CH_2O), 1.26 (bm, 14H, CH_2 × 7); ^{13}C NMR (100 MHz, $CDCl_3$, 300 K) δ (ppm) 172.5 (C═O), 156.2, 156.0 (C_{Ar}–O), 125.9 (CH_i25,27), 125.6 (CH_i26,28), 124.6, 123.9 (C_{Ar}–C), 96.9 (CH_e5,17), 96.0 (CH_e11,23), 64.3 (OCH_2), 56.0, 55.9 (OMe), 39.2 (CH_2–CO), 33.0 (CH), 28.7 (CH_2–CH_2O), 29.7, 29.1, 28.6, 28.4, 28.3, 28.1, 25.9 (7 δ CH_2). ESI-HRMS (positive) $C_{84}H_{124}O_{16}Na$ requires 1411.87816 (monoisotopic mass), m/z found 1411.87772 ($[M + Na]^+$. FT-IR (KBr) 2925, 2853, 1736, 1584, 1506, 1301, 1202 cm^{-1}.

Olefin Metathesis Reaction on Basket Resorc[4]arene 3b. Compound **3b** (0.134 g, 0.097 mmol) was dissolved in dry DCM (32 mL) to reach a final substrate concentration of 3.0 × 10^{-3} M. The solution was held at reflux temperature and then exposed to a solution of [$(H_2IMes)(PCy_3)(Cl)_2Ru$═CHPh)] catalyst (0.008 g, 0.0097 mmol, 10 mol %) in dry DCM (3 mL), previously prepared in the glovebox. The reaction mixture was kept at reflux under stirring and a nitrogen atmosphere for 40 min, and afterward treated with QuadraSil AP metal scavenger (aminopropyl silica gel, 1.5 g). After 5 min, the mixture was cooled to room temperature and left under stirring overnight. After filtration and evaporation, the residue was purified by silica gel chromatography with chloroform/methanol = 99:1 as the eluent to give compound **4b** (9 mg, 0.0032 mmol, 7%) and compound **5b** (13 mg, 0.0031 mmol, 10%). Starting material basket **3b** was recovered unreacted from the column eluted with DCM/ethyl acetate, 97:3 (30 mg, 23% by weight).

Crystallographic Data of Basket Resorc[4]arene 3b. $C_{84}H_{120}O_{16}$, M = 1385.862, triclinic crystal system, space group $P1$, a = 15.775(5) Å, b = 22.923(5) Å, c = 12.270(5) Å, α = 99.920(5)°, β = 111.030(5)°, γ = 81.180(5)°, volume 4059(2) Å^3, Z = 2, T = 293 K, ρ (calcd) = 1.134 g cm^{-3}, 14 527 total reflections collected, 13777 unique reflections (R_{int} = 0.06). Additional crystallographic data and experimental and refinement parameters are given in the Supporting Information.

UV–Visible Spectroscopic Experiments on Basket Resorc[4]-arene 3b. THF/water solutions of compound **3b** in the fixed concentration of 8.8 × 10^{-4} M were directly prepared in a quartz cuvette featuring THF/water ratios in the range of 1.326–0.538. In all

dx.doi.org/10.1021/jo502056v | J. Org. Chem. 2014, 79, 11051–11060

cases, the final volume of 1.0 mL was obtained by mixing 250 μL of a THF solution of **3b** (3.52×10^{-3} M) with 750 μL of a THF/water mixture progressively diluted in water. UV−visible absorptions at 261.0 and 284.5 nm of the different THF/water solutions analyzed are collected in Table 1S.

Molecular Mechanics Calculations. The superficial area of basket **3b** was assessed through Spartan '08 v. 1.2.0 software.[20] The analyzed geometry was the X-ray conformation after suitable optimization by molecular mechanics calculation based on the MMFF force field.

■ ASSOCIATED CONTENT

Supporting Information

CCDC 856088 contains the supplementary crystallographic data for this article (excluding structure factors) and can be obtained free of charge from The Cambridge Crystallographic Data Centre via http://www.ccdc.cam.ac.uk/data_request/cif. The supporting information related to this article includes the following: general experimental methods and copies of NMR spectra for compounds **2b**−**5b**, UV−visible spectroscopic data for basket resorc[4]arene; comparison of the physical descriptors found for basket resorc[4]arene **3b** with those previously found for fullerene derivatives **FD1**−**FD5**; linear correlation between $\Delta\Delta G_{cav}$ and $\%\Delta A$ values calculated for basket resorc[4]arene **3b** and fullerene derivatives **FD1**−**FD5**; and the CIF file for the X-ray data of basket resorc[4]arene **3b**. This material is available free of charge via the Internet at http://pubs.acs.org.

■ AUTHOR INFORMATION

Corresponding Authors

*E-mail: bruno.botta@uniroma1.it. Phone: +39-06-49912781. Fax: +39-06-49912780.

*E-mail: marco.pierini@uniroma1.it. Phone: +39-06-49912781. Fax: +39-06-49912780.

*E-mail: ilaria.dacquarica@uniroma1.it. Phone: +39-06-49912781. Fax: +39-06-49912780.

Notes

The authors declare no competing financial interest.

■ ACKNOWLEDGMENTS

We acknowledge financial support from the Center for Life NanoScience@LaSapienza, Istituto Italiano di Tecnologia (IIT), Roma, Italy (Funds 2011−2015); Sapienza Università di Roma, Italy (Funds for Selected Research Topics 2014−2015); and Bilateral Projects (2013−2014) between Sapienza Università di Roma (Italy) and Universidade Federal de Pernambuco (Brazil).

■ REFERENCES

(1) Wittenberg, J. B.; Isaacs, L. In *Supramolecular Chemistry: From Molecules to Nanomaterials*; Gale, P. A., Steed, J. W., Eds.; John Wiley & Sons: New York, 2012.

(2) Yamato, K.; Kline, M.; Gong, B. *Chem. Commun.* **2012**, *48*, 12142−12158.

(3) Li, X.; Upton, T. G.; Gibb, C. L. D.; Gibb, B. C. *J. Am. Chem. Soc.* **2003**, *125*, 650−651.

(4) Diederich, F., Stang, P. J., Eds. *Templated Organic Synthesis*; Wiley-VCH: Weinheim, Germany, 2000.

(5) (a) Chauvin, Y. *Angew. Chem., Int. Ed.* **2006**, *45*, 3740−3747. (b) Schrock, R. R. *Angew. Chem., Int. Ed.* **2006**, *45*, 3748−3759. (c) Grubbs, R. H. *Angew. Chem., Int. Ed.* **2006**, *45*, 3760−3765. (d) Vougioukalakis, G. C.; Grubbs, R. H. *Chem. Rev.* **2010**, *110*, 1746−1787. (e) Nicolaou, K. C.; Bulger, P. G.; Sarlah, D. *Angew. Chem., Int. Ed.* **2005**, *44*, 4490−4527.

(6) Pitarch, M.; McKee, V.; Nieuwenhuyzen, M.; McKervey, M. A. *J. Org. Chem.* **1998**, *63*, 946−951.

(7) (a) Hailu, S. T.; Butcher, R. J.; Hudrlik, P. F.; Hudrlik, A. M. *Acta Crystallogr., Sect. E: Struct. Rep. Online* **2012**, *68*, 1833−1834. (b) Hailu, S. T.; Butcher, R. J.; Hudrlik, P. F.; Hudrlik, A. M. *Acta Crystallogr., Sect. E: Struct. Rep. Online* **2013**, *69*, 1001−1002.

(8) (a) Cao, Y.; Wang, L.; Bolte, M.; Vysotsky, M. O.; Böhmer, V. *Chem. Commun.* **2005**, 3132−3134. (b) Vysotsky, M. O.; Bogdan, A.; Wang, L.; Böhmer, V. *Chem. Commun.* **2004**, 1268−1269.

(9) Yang, Y.; Swager, T. M. *Macromolecules* **2007**, *40*, 7437−7440.

(10) Ghirga, F.; D'Acquarica, I.; Delle Monache, G.; Toscano, S.; Mannina, L.; Sobolev, A. P.; Ugozzoli, F.; Crocco, D.; Antiochia, R.; Botta, B. *RSC Adv.* **2013**, *3*, 17567−17576.

(11) (a) Högberg, A. G. S. *J. Org. Chem.* **1980**, *45*, 4498−4500. (b) Högberg, A. G. S. *J. Am. Chem. Soc.* **1980**, *102*, 6046−6050. (c) Botta, B.; Cassani, M.; D'Acquarica, I.; Misiti, D.; Subissati, D.; Delle Monache, G. *Curr. Org. Chem.* **2005**, *9*, 337−355.

(12) Botta, B.; Delle Monache, G.; De Rosa, M. C.; Seri, C.; Benedetti, E.; Iacovino, R.; Botta, M.; Corelli, F.; Masignani, V.; Tafi, A.; Gacs-Baitz, E.; Santini, A.; Misiti, D. *J. Org. Chem.* **1997**, *62*, 1788−1794.

(13) Perrin, M.; Oehler, D. In *Calixarenes: A Versatile Class of Macrocyclic Compounds*; Vicens, J., Böhmer, V., Eds.; Kluwer Academic Publishers: Dordrecht, The Netherlands, 1991; pp 65−85.

(14) Botta, B.; D'Acquarica, I.; Delle Monache, G.; Nevola, L.; Tullo, D.; Ugozzoli, F.; Pierini, M. *J. Am. Chem. Soc.* **2007**, *129*, 11202−11212.

(15) Azov, V. A.; Beeby, A.; Cacciarini, M.; Cheetham, A. G.; Diederich, F.; Frei, M.; Gimzewski, J. K.; Gramlich, V.; Hecht, B.; Jaun, B.; Latychevskaia, T.; Lieb, A.; Lill, Y.; Marotti, F.; Schlegel, A.; Schlittler, R. R.; Skinner, P. J.; Seiler, P.; Yamakoshi, Y. *Adv. Funct. Mater.* **2006**, *16*, 147−156.

(16) Angelini, G.; Cusan, C.; De Maria, P.; Fontana, A.; Maggini, M.; Pierini, M.; Prato, M.; Schergna, S.; Villani, C. *Eur. J. Org. Chem.* **2005**, 1884−1891.

(17) The dependency of API on substrate concentration (namely, [S]) is shown by the following formula: $API^2 = p \times \log [S] + C$, where p and C are the slope and the intercept, respectively, of a straight line experimentally derived.

(18) $\kappa\gamma = 9.00 \times 10^{-16}\ e^{(\delta_H/0.78319)} + 2.00 \times 10^{-4}\ e^{(\delta_H/6.27152)} + 5.61 \times 10^{-3}$. See reference 16 for further details.

(19) (a) Prato, M. *J. Mater. Chem.* **1997**, *7*, 1097−1109. (b) Da Ros, T.; Prato, M. *Chem. Commun.* **1999**, 663−669. (c) Brabec, C. J.; Cravino, A.; Meissner, D.; Sariciftci, N. S.; Fromherz, T.; Rispens, M. T.; Sanchez, L.; Hummelen, J. C. *Adv. Funct. Mater.* **2001**, *11*, 374−380. (d) Chawla, P.; Chawla, V.; Maheshwari, R.; Saraf, S. A.; Saraf, S. K. *Mini-Rev. Med. Chem.* **2010**, *10*, 662−677.

(20) *Spartan '08*, v.1.2.0; Wavefunction, Inc.: Irvine, CA, 2008.